

This is the accepted manuscript made available via CHORUS. The article has been published as:

Transport spin polarization of high Curie temperature MnBi films

P. Kharel, P. Thapa, P. Lukashev, R. F. Sabirianov, E. Y. Tsymbal, D. J. Sellmyer, and B. Nadgorny

Phys. Rev. B **83**, 024415 — Published 31 January 2011

DOI: [10.1103/PhysRevB.83.024415](https://doi.org/10.1103/PhysRevB.83.024415)

Transport Spin Polarization of High-Curie Temperature MnBi Films

P. Kharel,^{1,2} P. Thapa,³ P. Lukashev,^{1,2} R. F. Sabirianov,^{4,2}
E. Y. Tsymbal,^{1,2} D. J. Sellmyer,^{1,2} and B. Nadgorny³

¹*Department of Physics and Astronomy,
University of Nebraska - Lincoln, Lincoln, NE, 68588*

²*Nebraska Center for Materials and Nanoscience,
University of Nebraska - Lincoln, Lincoln, Nebraska 68588*

³*Department of Physics and Astronomy,
Wayne State University, Detroit, MI, 48201*

⁴*Department of Physics, University of Nebraska at Omaha, Omaha, NE 68182*

(Dated: December 13, 2010)

Abstract

We report on the study of the structural, magnetic and transport properties of highly textured MnBi films with the Curie temperature of 628K. In addition to detailed measurements of resistivity and magnetization, we measure transport spin polarization of MnBi by Andreev reflection spectroscopy and perform fully relativistic band structure calculations of MnBi. A spin polarization from 51 ± 1 to $63\pm 1\%$ is observed, consistent with the calculations and with an observation of a large magnetoresistance in MnBi contacts. The band structure calculations indicate that, in spite of almost identical densities of states at the Fermi energy, the large disparity in the Fermi velocities leads to high transport spin polarization of MnBi. The correlation between the values of magnetization and spin polarization is discussed.

I. INTRODUCTION

Successful implementation of many novel concepts and devices in spintronics is largely dependent on our ability to controllably generate and inject electronic spins, preferably at room temperature¹, which require spin injectors to combine high Curie temperature with reasonably high conductivity. Unlike all-metal devices, where efficient electrical spin injection has been demonstrated², spin injection from ferromagnetic metals into semiconductors proved to be more challenging, partly because of the low interface resistance³. This problem may be circumvented by spin injection from 100% spin polarized, half-metallic contacts, tunnel contacts, or semiconductor contacts. While a number of promising magnetic semiconducting systems, such as (Ga,Mn)As, for example, have been investigated⁴, their relatively low Curie temperatures make practical implementation of these materials difficult. Doping some of the magnetic oxides with magnetic ions represents another approach; however, the progress in this area has been slow due in part to persisting reproducibility problems⁵.

The interest in ferromagnetic MnBi stems from its high Curie temperature, which is well above room temperature⁶, high coercivity with a rectangular hysteresis loop⁷, large perpendicular room-temperature anisotropy in thin films⁸ that can be used as spin injectors for spin lasers and spin emitting diodes⁹, and an extraordinarily large Kerr rotation¹⁰. The ferromagnetic phase in the NiAs structure is the most stable at room temperature, undergoing a coupled structural and magnetic phase transition at 628K. These unusual magnetic and magneto-optical properties have been the main motivation for the intensive studies on the various properties of this material¹¹. Recently it has been predicted that MnBi in the hypothetical zinc blende structure is fully half-metallic¹²⁻¹⁴. The experimental implementation of the zinc blende MnBi may be quite challenging - not only because it is difficult to grow MnBi epitaxially, but also because the zinc blende phase may be metastable. On the other hand, MnBi in the NiAs structure can be fabricated, is ferromagnetic up to 628 K, and is a fairly good conductor at room temperature. Moreover, the properties of MnBi interface may be controlled by the addition of Bi, which shows a semimetal-semiconductor transition at small thicknesses¹⁵. From this perspective it is particularly important to measure the transport spin polarization of MnBi in the NiAs structure, which is also relevant to the understanding of MnBi junctions that show a large magnetoresistance (70% at room temperature)¹⁶.

The question of maximizing the value of the transport spin polarization P_T is often dis-

cussed in the context of possible correlation of P_T with the value of magnetization M , or the average atomic magnetic moment of a ferromagnet. Experimentally, while the linear relationship between P_T and M has been reported¹⁷, in many other cases no direct relationship between the two quantities has been observed^{18–20}. As P_T is associated with the electronic states near the Fermi energy and the respective Fermi velocities, whereas the magnetic moment is associated with the algebraic sum of occupancies of all majority and minority spin states, there is no reason for these quantities to be related. Thus the determination of whether or not the link between the two quantities exists in a concrete materials system has to be made independently.

Here we report the Point Contact Andreev Reflection (PCAR)^{21,22} measurements of the transport spin polarization, P_T of MnBi thin films in the NiAs crystallographic structure. We find a relatively large spin polarization of up to 63%, consistent with our density functional calculations and an observation of a large magnetoresistance in MnBi contacts¹⁶. We also report a correlation between the values of the saturation magnetization and the transport spin polarization.

II. EXPERIMENTAL PROCEDURE

MnBi thin films were prepared by sequential evaporation of Bi and Mn onto a glass substrate using an e-beam evaporator with subsequent *in situ* annealing of bi-layers immediately after the deposition. High quality MnBi thin films can be grown by this method, if the Mn to Bi atomic ratio of 55 to 45 is maintained during deposition²³. Here we will present the data taken on four samples with the thicknesses from approximately 32 nm (samples A, C, and D) to 47 nm (sample B). Two samples (A and C) were deposited at room temperature and annealed for one hour at 410°C and 400°C respectively; the other two samples (B and D) were deposited at 125°C and annealed at 350°C for one and a half and one hour respectively. All of the samples were single phase MnBi highly textured polycrystalline films, with a hexagonal NiAs crystal structure, although small traces of elemental Bi have been detected (see Fig. 1).

Depending on the experiment, several generally different definitions of spin polarization has been introduced²⁴. P_T is defined as $P_{N_v} = \frac{\langle Nv \rangle_{\uparrow} - \langle Nv \rangle_{\downarrow}}{\langle Nv \rangle_{\uparrow} + \langle Nv \rangle_{\downarrow}}$, or as $P_{N_{v^2}} = \frac{\langle Nv^2 \rangle_{\uparrow} - \langle Nv^2 \rangle_{\downarrow}}{\langle Nv^2 \rangle_{\uparrow} + \langle Nv^2 \rangle_{\downarrow}}$ in the case of the ballistic and diffusive regimes respectively, where v is the Fermi velocity, and

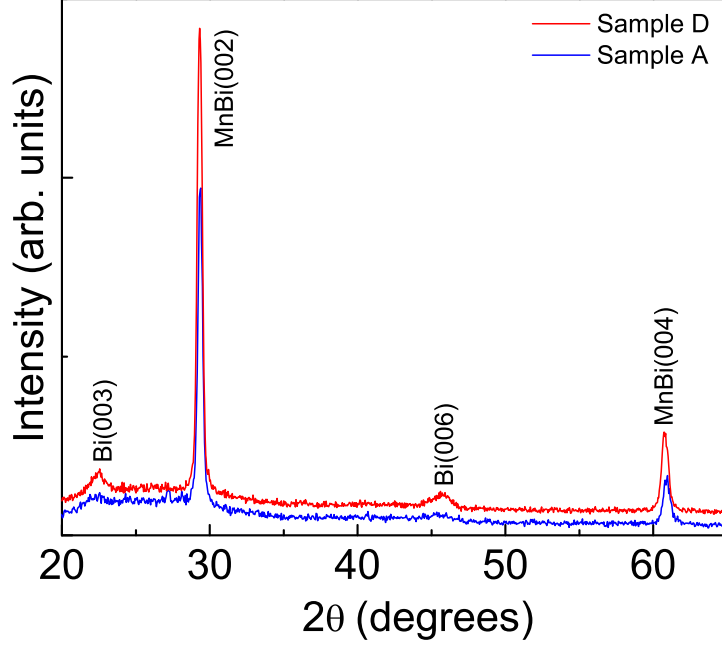


FIG. 1: (Color online). XRD spectra of MnBi film (samples A and D). Strong diffraction peaks from (002) and (004) planes show preferred c-axis orientation of the films.

N is the spin-projected densities of states (DOS) for majority (\uparrow) and minority (\downarrow) spins respectively. In the ballistic regime only one component of velocity predominantly enters the averaging. For all of the point contact measurements described here electrochemically etched Nb tips were used²⁵. The differential conductance dI/dV was obtained by a four-probe technique with standard ac lock-in detection at a frequency of approximately 2 kHz. The details of the experimental techniques and the data analysis can be found in the paper of Panguluri *et. al.*²⁶. Since, as we will show below, all the contacts are largely in the ballistic regime, we used the modified Blonder-Tinkham-Klapwijk (BTK)²⁵ model²⁷ in the ballistic regime to analyze the data. The typical conductance curves for samples A, B, C, and D are shown in Fig. 2a. To account for possible empirical Z^2 dependence of the spin polarization values on a scattering parameter Z at the F/S interface, often encountered in the PCAR measurements²⁸, we plotted $P(Z)$ dependencies for the respective samples in Fig. 2b taking the extrapolation of the least square fit to the case of transparent interface ($Z = 0$) to obtain the limiting values of P_T . This procedure resulted in spin polarizations of 63 ± 0.8 , 57.8 ± 1.6 ,

54.2±2.4, and 51.7±1.1%, for samples A, B, C, and D respectively.

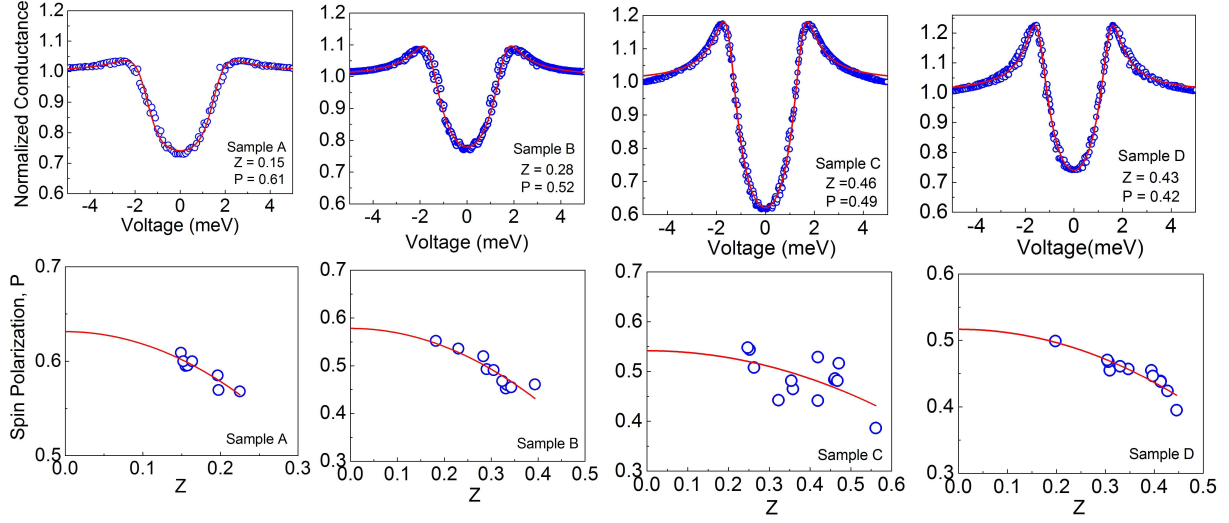


FIG. 2: (Color online). (a) Top panel: Examples of normalized conductance curves for samples A, B, C, and D. Sample A: contact resistance $R_C = 36.1 \Omega$, the fitting parameters $Z = 0.15$ and $P = 61\%$; Sample B: $R_C = 50.5 \Omega$, $Z = 0.28$ and $P = 52\%$. Sample C: $R_C = 28.8 \Omega$, $Z = 0.46$, $P = 49\%$; Sample D: $R_C = 17.9 \Omega$, $Z = 0.43$ and $P = 42.4\%$; The BCS gap of niobium $\Delta = 1.5$ meV is used. (b) Bottom panel: $P(Z)$ dependence for samples A, B, C, and D respectively. The size of the data points corresponds to the error bars in Z and $P \sim 0.02$.

III. EXPERIMENTAL RESULTS

We find that the values of the spin polarization are correlated with the magnetic properties of MnBi films. Magnetic hysteresis curves show that the samples are highly anisotropic with the magnetization easy axis perpendicular to the sample plane, with very high values of uniaxial anisotropy constants K_1 and K_2 , consistent with the previous reports²³. While all of the samples show well defined, rectangular hysteresis loops in the out of plane geometry (see top left inset in Fig. 3), the magnetization and coercivity seem to be very sensitive to the sample preparation conditions. Specifically, the measured saturation magnetizations are 503, 485, 464 and 425 emu/cm³ and coercivities are 8.4, 3.2, 7.9 and 5.4 kOe at 300 K for the samples A, B, C, and D respectively. As can be seen from Fig. 3 the experimental values of P_T correlate with the values of the saturation magnetization of MnBi²⁹. We attribute this

behavior to magnetic disorder which may have adverse effects on the values of magnetization and spin polarization, as has been reported for SrFeMoO_6 , for example³⁰. We discuss this behavior below in view of our first-principles calculations.

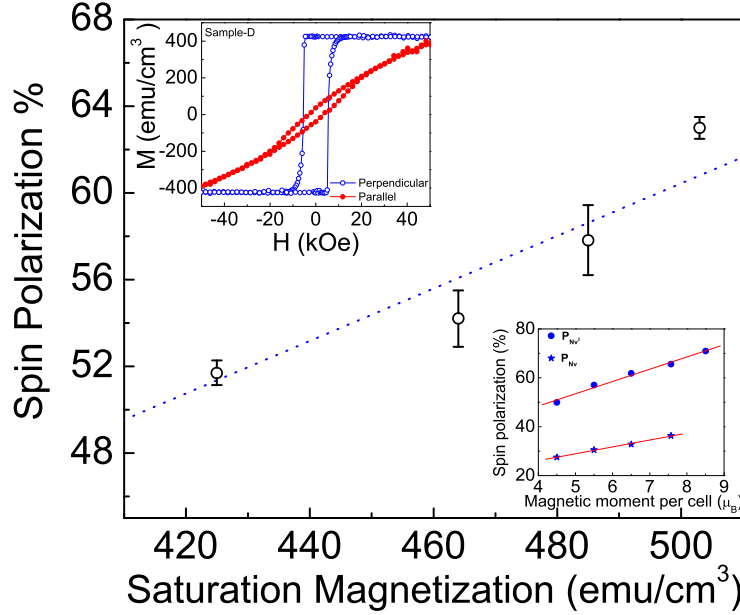


FIG. 3: Spin polarization P vs. saturation magnetization M_s for samples A, B, C, and D. The straight line is constrained to go through the origin. Top inset: $M(H)$ loop for sample D in the magnetic field parallel and perpendicular to the c -axis. Bottom inset: calculated spin polarization vs. magnetic moment per MnBi unit cell.

All MnBi samples are metallic and exhibit a qualitatively similar temperature dependence of the resistivity ρ from 2 to 300 K (see Fig. 4). The residual resistance ratio ρ_{RT}/ρ_{4K} is almost the same (~ 8.5) for all the samples, with $\rho_{4K} \sim 15 \mu\Omega\text{cm}$. Surprisingly, we found that the low temperature ($4K < T < 30K$) resistivity of all the samples follow an anomalous power law, different from the $\rho \sim T^2$ expected for weakly ferromagnetic metals, due to a single magnon scattering mechanism³¹. The resistivity of our samples follow the $\rho \sim T^m$ power law with m between 2.9 and 3.6, similarly to what has been observed in some half-metallic films, such as CrO_2 ³². While it has been suggested that the T^3 power law may be related to the unconventional single magnon scattering mechanism in half metals due to the spin fluctuations at finite temperatures³³, our results on MnBi indicate that it cannot be considered a definitive test for half-metallicity.

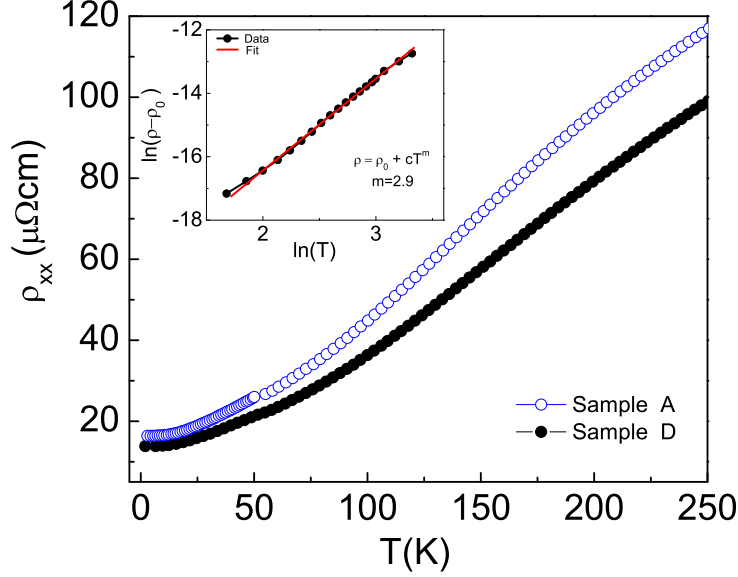


FIG. 4: (Color online). Resistivity of MnBi film as a function of temperature (samples A and D), showing the metallic behavior with the residual resistivity of $15 \mu\Omega\text{cm}$. Inset: The power law dependence $\rho \sim T^m$ at low temperatures (below 30 K) with $m = 2.9$.

IV. COMPUTATIONAL RESULTS

To interpret the measured values of spin polarization we have implemented electronic band structure calculations of bulk MnBi in the NiAs phase, using the tight-binding linear muffin-tin orbital (TB-LMTO) method³⁴, within the local density approximation (LDA). We performed fully relativistic calculations, i.e. the scalar relativistic wave equation is solved. To explore the role of spin-orbit interaction (SO), we carried out the calculations both with and without taking spin orbit coupling into account. Somewhat surprisingly, we find that SO practically does not affect our results (see Fig. 5 and Fig. 6). While there is a slight band shift on the order of SO constant (Fig. 5), we found practically no difference in the total calculated DOS. Close inspection also shows that the inclusion of SO does not significantly change the dispersion relationships at the Fermi level (Fig. 6). Consequently the Fermi velocities - and thus the values of transport spin polarization would only be marginally affected by the inclusion of the SO coupling.

Fig. 7 (top panel, shaded region) shows that the total densities of states (DOS) at the

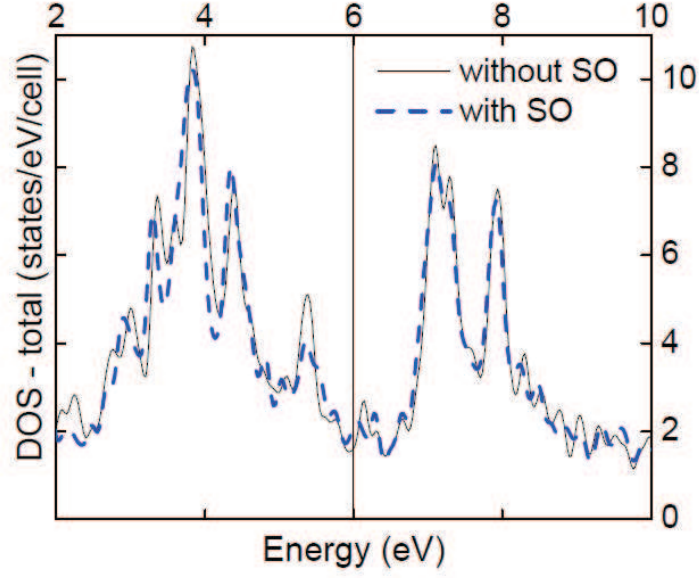


FIG. 5: (Color online). Comparison between the DOS without SO (solid black line) and with SO (dashed blue line).

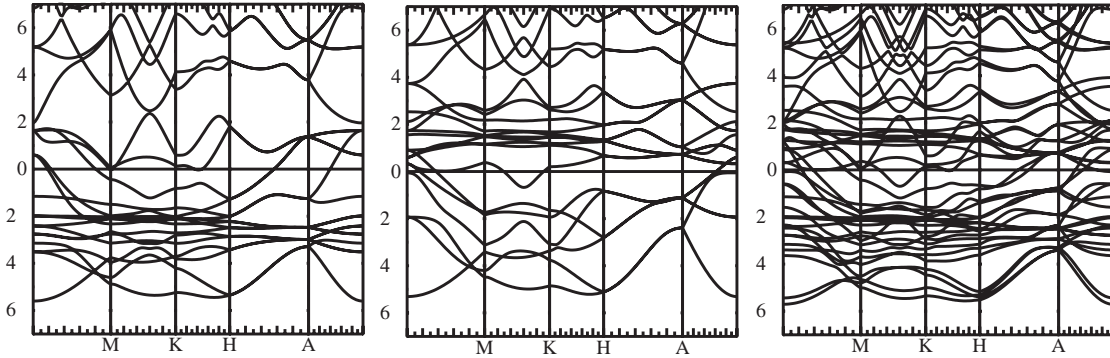


FIG. 6: Energy bands for majority spin channel without SO (left panel), minority spin channels without SO (middle panel), both majority and minority spin channels with SO (right panel).

Fermi energy are nearly equal (~ 0.45 states/cell/eV) for majority- and minority-spin carriers, resulting in a vanishing spin polarization, $P_N = \frac{N_\uparrow - N_\downarrow}{N_\uparrow + N_\downarrow}$, where N_\uparrow and N_\downarrow are the majority- and minority-spin DOS (see bottom panel of the Fig. 7). The origin of the large P_T measured in MnBi is due to the substantial spin asymmetry of the electronic bands near the Fermi energy. The close inspection of the dispersion of the minority and majority bands

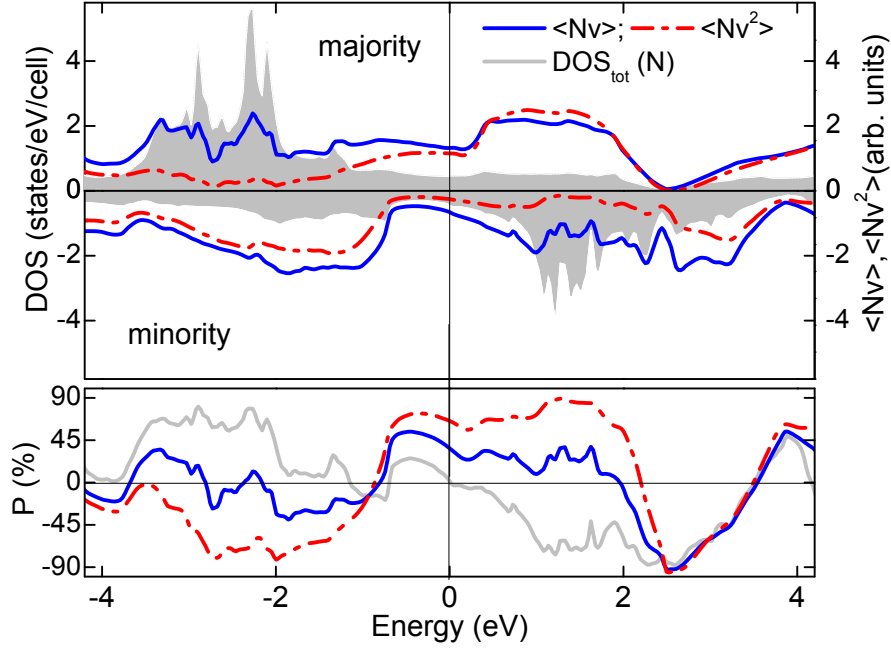


FIG. 7: (Color online). Top panel - total DOS for majority and minority carriers (shaded region), $\langle Nv \rangle_{\uparrow(\downarrow)}$ (blue solid line), $\langle Nv^2 \rangle_{\uparrow(\downarrow)}$ (dashed red line); bottom panel - P near the Fermi energy for P_N (DOS) (black solid line crossing zero at 0 eV), P_{Nv} (solid blue line), and P_{Nv^2} (dashed red line) in the direction of the c -axis. Inclusion of spin - orbit coupling (from fully relativistic calculations) practically does not affect the calculated DOS as seen in Fig. 5.

(see Fig. 8) indicates that the minority spin states have a lower Fermi velocity compared to the majority bands. Indeed, the calculated Fermi velocities $v_{\uparrow(\downarrow)}$ are 1.2×10^6 and 0.6×10^6 m/s for the majority and minority bands respectively (both are almost constant in the range ± 0.5 eV around E_F). Thus, when the mobility of electrons is taken into account, a large P_T is expected^{35–37}. The definition of P_T in the diffusive regime assumes that the relaxation time which enters the expression for the conductivity is spin-independent³⁷. This may be qualitatively justified given the fact that the relaxation time is proportional to the DOS at the Fermi energy³⁸, but the latter is nearly spin-independent according to our calculations. The calculations yield the spin polarization $P_{Nv} = 36\%$ and $P_{Nv^2} = 66\%$ assuming that the Fermi velocity is projected to the c -axis (perpendicular to the plane of the film). Both P_{Nv} and P_{Nv^2} are reduced for the velocity direction perpendicular to the c -axis, i.e. in the ab -plane ($P_{Nv} = 28\%$ and $P_{Nv^2} = 51\%$). This implies that lower values of spin polarization

are expected for polycrystalline MnBi samples due to the strong anisotropy of transport properties of MnBi.

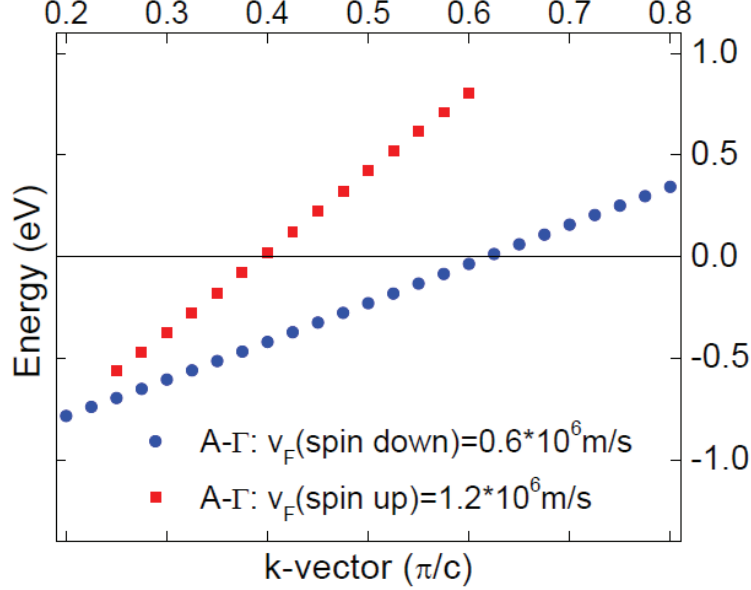


FIG. 8: (Color online). Dispersion of the minority and majority bands near Fermi level. Blue spheres - minority band; red squares - majority band.

To examine the correlation between saturation magnetization and spin polarization we used the fixed-spin moment method³⁹. The results shown in Fig. 3 (bottom inset) indicate an approximately linear relationship between P_T and the magnetic moment. This behavior is the consequence of nearly linear variation of the exchange splitting of the spin bands with the magnetic moment. Experimentally, the variation of the saturation magnetization may be due to a different degree of structural disorder in our samples. As follows from our calculations⁴⁰, placing Mn atoms in the interstitial sites leads to the antiferromagnetic alignment of their moments with the moments of the Mn atoms in the regular sites. The magnetization of MnBi decreases together with the value of spin polarization, supporting the experimentally observed trend in our MnBi samples.

V. DISCUSSION AND CONCLUSION

Using the measured value of the resistivity of MnBi ($\sim 15 \mu\Omega \text{ cm}$ at 4 K) and the calculated density of states, $N_{\uparrow} = 0.446$ and $N_{\downarrow} = 0.425$ states/eV/cell, we estimate the mean free path for majority (\uparrow) and minority (\downarrow) carriers from the Ziman formula $\sigma_{\uparrow(\downarrow)} = 1/3e^2N_{\uparrow(\downarrow)}v_{F\uparrow(\downarrow)}^2\tau$, $L_{\uparrow} \approx 20nm$, $L_{\downarrow} \approx 10nm$. Using Wexler's formula⁴¹ $R_c \approx 4\rho L/3\pi d^2 + \rho/2d$ the contact size can be estimated from 5 - 15 nm depending on the contact resistance, $10\Omega < R_C < 100\Omega$, indicating that the transport is in the ballistic regime for majority carriers and in the intermediate regime ($d \sim L$) for minority carriers. While these estimates suggest that our conditions correspond to the ballistic regime, our experimental results yield a better agreement with the theoretical calculations in the diffusive ($P_{Nv^2} = 51 - 66\%$), rather than in the ballistic ($P_{Nv} = 28 - 36\%$) limit. A possible explanation is that the spin polarization can often be very sensitive to the interface, and to the termination of electrodes⁴². In MnBi it is expected to be strongly dependent on the surface termination because of the substantial difference in the electronic DOS at the Fermi energy for Bi and Mn. We find that P_T is enhanced assuming the Bi states control the magnitude of P ($P_{Nv} = 55\%$ and $P_{Nv^2} = 76\%$ respectively).

In conclusion, we have investigated the structural, magnetic and transport properties of high Curie temperature MnBi films. A transport spin polarization was measured using the Point Contact Andreev Reflection technique and values up to 63% are obtained, consistent with observations of a large magnetoresistance in MnBi contacts and the results of band structure calculations. Our first-principles calculations indicate that, in spite of almost identical densities of states at the Fermi energy in the majority- and minority-spin bands, the large disparity in the Fermi velocities results in a high transport spin polarization of MnBi. Our experimental data and first-principles calculations show a nearly linear relationship between the values of P_T and the magnetic moment (magnetization) of MnBi.

VI. ACKNOWLEDGEMENTS

The work at University of Nebraska was supported by NSF-MRSEC (grant No. DMR-0820521), DOE (grant # DE-FG02-04ER46152), NSF-EPS (grant No. EPS-1010674), the Nebraska Research Initiative, and NCMN. The work at Wayne State was supported by the

NSF CAREER ECS-0239058 and the ONR grant N00014-06-1-0616. We thank Mark van Schilfgaarde for providing the tight-binding LMTO code; we also thank Kirill Belashchenko and Alexander Wysocki for helpful discussions.

-
- ¹ I. Zutic, J. Fabian, and S. Das Sarma, *Rev. Mod. Phys.* **76**, 323 (2004).
 - ² M. Johnson, and R. H. Silsbee, *Phys. Rev. Lett.* **55**, 1790 (1985); F. J. Jedema, A. T. Filip, and B. J. van Wees, *Nature* **410**, 345 (2001).
 - ³ P. C. van Son, H. van Kempen, and P. Wyder, *Phys. Rev. Lett.* **58**, 2271 (1987); G. Schmidt et al., *Phys. Rev. B* **62**, R4790 (2000).
 - ⁴ H. Ohno, A. Shen, F. Matsukura, A. Oiwa, A. Endo, S. Katsumoto, and Y. Iye, *Appl. Phys. Lett.* **69**, 363 (1996); A. H. MacDonald, P. Schiffer, and N. Samarth, *Nature Mater.* **4**, 195 (2005).
 - ⁵ J. M. D. Coey, *Current Opinion in Solid State and Materials Science* **10**, 83(2006); A. Zunger, S. Lany, H. Raebiger, *Physics* **3**, 53 (2010); K. Sato et al., *Rev. Mod. Phys.* **82**, 1633 (2010); S. A. Chambers, *Adv. Materials* **22**, 219 (2010).
 - ⁶ R. R. Heikes, *Phys. Rev.* **99**, 446 (1955).
 - ⁷ X. Guo, X. Chen, Z. Altounian and J. O. Strm-Olsen, *J. Appl. Phys.* **73**, 6275 (1993).
 - ⁸ U. Rüdiger and G. Güntherodt, *J. Appl. Phys.* **88**, 4221(2000).
 - ⁹ M. Holub, J. Shin, D. Saha, and P. Bhattacharya, *Phys. Rev. Lett.* **98**, 146603 (2007); C. Göthgen, R. Oszwaldowski, A. Petrou, and I. Zutic, *Appl. Phys. Lett.* **93**, 042513 (2008).
 - ¹⁰ G. Q. Di, S. Iwata, S. Tsunashima, and S. Uchiyama, *J. Magn. Magn. Mater.* **104**, 1023 (1992).
 - ¹¹ A. Katsui, *J. Appl. Phys.* **47**, 4663 (1976); J. X. Shen, R. D. Kirby, and D. J. Sellmyer, *J. Appl. Phys.* **69**, 5984 (1991); S. S. Jaswal, J. X. Shen, R. D. Kirby, and D. J. Sellmyer, *J. Appl. Phys.* **75**, 6346 (1994); J. Köhler and J. Kübler, *J. Phys.: Condens. Matter* **8**, 8681 (1996); U. Rüdiger, et. al., *IEEE Trans. Magn.* **33**, 3241 (1997); P. R. Bandaru and T. D. Sands, *J. Appl. Phys.* **86**, 1596 (1999).
 - ¹² Y. Q. Xu, B. G. Liu, and D. G. Pettifor, *Phys. Rev. B* **66**, 184435 (2002).
 - ¹³ J. Zheng and J. W. Davenport, *Phys. Rev. B* **69**, 144415 (2004).
 - ¹⁴ L. Kahal and M. Ferhat, *J. Appl. Phys.* **107**, 043910 (2010).
 - ¹⁵ E.I. Rogacheva, et. al., *Thin Solid Films*, **31**, 3411 (2008).

- ¹⁶ E. Clifford, M. Venkatesan and J. M. D. Coey, *J. Magn. Magn. Mater.* **272-276**, 1614 (2004).
- ¹⁷ R. Meservey and P. M. Tedrow, *Phys. Rep.* **238**, 173 (1994).
- ¹⁸ R. J. M. Veerdonk, J. S. Moodera, and W. J. M. de Jonge, *Conf. Digest of the 15th Int. Colloquium on Magnetic Films and Surfaces*, Queensland, Aug. 1997.
- ¹⁹ C. Kaiser, S. van Dijken, S.-H. Yang, H. Yang, and S. S. P. Parkin, *Phys. Rev. Lett.* **94**, 247203 (2005).
- ²⁰ B. Nadgorny, R. J. Soulen, Jr., M. S. Osofsky, I. I. Mazin, G. Laprade, R. J. M. van de Veerdonk, A. A. Smits, S. F. Cheng, E. F. Skelton, and S. B. Qadri, *Phys. Rev. B* **61**, R3788 (2000).
- ²¹ R. J. Soulen, Jr., J. M. Byers, M. S. Osofsky, B. Nadgorny, T. Ambrose, S. F. Cheng, P. R. Broussard, C. T. Tanaka, J. Nowak, J. S. Moodera, A. Barry and J. M. D. Coey, *Science* **282**, 85 (1998).
- ²² S. K. Upadhyay, A. Palanisami, R. N. Louie, and R. A. Buhrman, *Phys. Rev. Lett.* **81**, 3247 (1998).
- ²³ P. Kharel, R. Skomski, R. D. Kirby, and D. J. Sellmyer, *J. Appl. Phys.* **107**, 09E303 (2010).
- ²⁴ I. I. Mazin, *Phys. Rev. Lett.* **83**, 1427 (1999); J. P. Velev, et. al., *Surface Science Reports* **63**, 400 (2008).
- ²⁵ G. E. Blonder, M. Tinkham, and T. M. Klapwijk, *Phys. Rev. B* **25**, 4515 (1982).
- ²⁶ R. P. Panguluri, G. Tsoi, B. Nadgorny, S. H. Chun, N. Samarth, and I. I. Mazin, *Phys. Rev. B* **68**, 201307(R) (2003).
- ²⁷ I. I. Mazin, A. A. Golubov, and B. Nadgorny, *J. Appl. Phys.* **89**, 7576 (2001).
- ²⁸ G. T. Woods, R. J. Soulen Jr., I. Mazin, B. Nadgorny, M. S. Osofsky, J. Sanders, H. Srikanth, W. F. Egelhoff, and R. Datla, *Phys. Rev. B* **70**, 054416 (2004); Y. Ji, G. J. Strijkers, F. Y. Yang, C. L. Chien, J. M. Byers, A. Anguelouch, G. Xiao, and A. Gupta, *Phys. Rev. Lett.* **86**, 5585 (2001).
- ²⁹ As unreacted Bi is likely to be present next to the substrate, it will not affect the transport properties of the film, but can complicate the exact determination of the magnetization.
- ³⁰ R. P. Panguluri, S. Xu, Y. Moritomo, Y. I. Solovyev, and B. Nadgorny, *Appl. Phys. Lett.* **94**, 012501 (2009).
- ³¹ I. Mannari, *Prog. Theor. Phys.* **22**, 335 (1959).
- ³² A. Gupta, X. W. Li, and G. Xiao, *J. Appl. Phys.* **87**, 6073 (2000).
- ³³ N. Furukawa, *J. Phys. Soc. Jpn.* **69**, 1954 (2000).

- ³⁴ O. K. Andersen, *Phys. Rev. B* **12**, 3060 (1975).
- ³⁵ Similar to SrRuO₃, *e.g.*, B. Nadgorny, *et. al.*, *Appl. Phys. Lett.* **82**, 427 (2003).
- ³⁶ I. I. Mazin, *Phys. Rev. Lett.* **83**, 1427 (1999).
- ³⁷ J. P. Velev, P. A. Dowben, E. Y. Tsymbal, S. J. Jenkins, and A. N. Caruso, *Surface Science Reports* **63**, 400 (2008).
- ³⁸ E. Y. Tsymbal and D. G. Pettifor, Perspectives of giant magnetoresistance, in *Solid State Physics*, edited by H. Ehrenreich and F. Spaepen, Vol. **56** (Academic Press, 2001) pp.113-237.
- ³⁹ V. L. Moruzzi, P. M. Marcus, K. Schwarz, and P. Mohn, *Phys. Rev.* **34**, 1784 (1986).
- ⁴⁰ P. Kharel, R. Skomski, P. Lukashev, R. F. Sabirianov, and D. J. Sellmyer, *submitted*.
- ⁴¹ Wexler, *Proc. Phys. Soc. London* **89**, 927 (1966)]
- ⁴² E. Y. Tsymbal, K. D. Belashchenko, J. Velev, S. S. Jaswal, M. van Schilfgaarde, I. I. Oleynik, and D. A. Stewart, *Prog. Mater. Science* **52**, 401 (2007).